THE GERONTOLOGICAL SOCIETY OF AMERICA®

Journals of Gerontology: Biological Sciences
cite as: *J Gerontol A Biol Sci Med Sci*, 2023, Vol. 78, No. 8, 1339–1347
https://doi.org/10.1093/gerona/glad080
Advance Access publication March 5, 2023

OXFORD

Original Article

Lower Myelin Content Is Associated With Lower Gait Speed in Cognitively Unimpaired Adults

Mary E. Faulkner, BS,[1] John P. Laporte, BS,[1] Zhaoyuan Gong, PhD,[1] Mohammad A. B. S. Akhonda, PhD,[1] Curtis Triebswetter, MS,[1] Matthew Kiely, BS,[1,•] Elango Palchamy, PhD,[2] Richard G. Spencer, MD, PhD,[1] and Mustapha Bouhrara, PhD[1,*]

[1]Laboratory of Clinical Investigation, National Institute on Aging, National Institutes of Health, Baltimore, Maryland, USA. [2]Translational Gerontology Branch, National Institute on Aging, National Institutes of Health, Baltimore, Maryland, USA.

*Address correspondence to: Mustapha Bouhrara, PhD, Magnetic Resonance Physics of Aging and Dementia Unit, Laboratory of Clinical Investigation, National Institute on Aging, National Institutes of Health, BRC 05C-222, 251 Bayview Boulevard, Baltimore, MD 21224, USA. E-mail: bouhraram@mail.nih.gov

Received: November 22, 2022; Editorial Decision Date: March 1, 2023

Decision Editor: David Le Couteur, MBBS, FRACP, PhD

Abstract

Mounting evidence indicates that abnormal gait speed predicts the progression of neurodegenerative diseases, including Alzheimer's disease. Understanding the relationship between white matter integrity, especially myelination, and motor function is crucial to the diagnosis and treatment of neurodegenerative diseases. We recruited 118 cognitively unimpaired adults across an extended age range of 22–94 years to examine associations between rapid or usual gait speeds and cerebral myelin content. Using our advanced multicomponent magnetic resonance relaxometry method, we measured myelin water fraction (MWF), a direct measure of myelin content, as well as longitudinal and transverse relaxation rates (R_1 and R_2), sensitive but nonspecific magnetic resonance imaging measures of myelin content. After adjusting for covariates and excluding 22 data sets due to cognitive impairments or artifacts, our results indicate that participants with higher rapid gait speed exhibited higher MWF, R_1, and R_2 values, that is, higher myelin content. These associations were statistically significant within several white matter brain regions, particularly the frontal and parietal lobes, splenium, anterior corona radiata, and superior fronto-occipital and longitudinal fasciculus. In contrast, we did not find any significant associations between usual gait speed and MWF, R_1, or R_2, which suggests that rapid gait speed may be a more sensitive marker of demyelination than usual gait speed. These findings advance our understanding on the implication of myelination in gait impairment among cognitively unimpaired adults, providing further evidence of the interconnection between white matter integrity and motor function.

Keywords: Aging, Gait speed, MRI, Myelin, Relaxation rates

Gait speed is a functional measure that reflects performance status of a wide range of physiologic systems and functions, integrating muscle strength, balance, proprioception, motivation, vision, weight, joint mobility, as well as cardiovascular and pulmonary functions (1). Indeed, it has emerged as a single biomarker for health status (2), including survival itself (3). There is growing evidence suggesting that the decline in gait speed with aging reflects progressive neurodegeneration (4,5). This interpretation is consistent with studies showing slowing of motor function, as reflected by impairment of gait, may precede the onset of overt cognitive decline and Alzheimer's disease (AD) as well as other dementias (6,7). In particular, the relationship between neurodegeneration and abnormal gait speed is thought to reflect age-related changes in the micro- and macro-structures of both gray and white matters. Indeed, neuroimaging studies across a range of modalities and experimental designs have shown that the development of abnormal gait speed, as well as other issues in locomotor and postural stability, is associated with greater gray matter atrophy (8), white matter hyperintensities (9), in addition to β-amyloid burden, a neuropathological hallmark of AD (10). These changes in gray and white matter tend to be localized in cortical tissue related to executive function and motor planning including the prefrontal cortex, supplementary motor regions, and cerebellum, as well as in subcortical white tissue tracts that carry executive and sensorimotor information, such as proprioception and vision, to lower brain centers (11,12).

White matter tissue integrity is commonly assessed by measuring white matter lesions with structural T_2/fluid attenuated inversion recovery magnetic resonance imaging (MRI) or by measuring white matter microstructural alterations with diffusion tensor imaging (DTI). Several studies based on structural imaging and DTI have examined the effects of white matter microstructural differences on gait speed in healthy and pathological cognitive aging. For instance, Snir et al. studied white matter tract regions, including the corpus callosum, forceps major and minor, longitudinal fasciculus, fronto-occipital fasciculus, and the corticospinal tract (11); they found that, among individuals with mild cognitive impairment (MCI), DTI parameters—namely, fractional anisotropy, mean diffusivity, axial diffusivity, and radial diffusivity, which probe water mobility and tissue integrity and architecture—were correlated with slower gaits. Other studies have reported similar correlations between structural MRI or DTI metrics and gait stability (12), frailty (13,14), lap time variability (15), and physical activity (16,17). While these studies offer compelling evidence that loss of white matter integrity is associated with impaired gait performance in adults, especially those with neurodegenerative diseases, they are fundamentally limited by the inability of conventional structural imaging or DTI techniques to specifically determine whether abnormalities in white matter microstructure reflect differences in axonal density or myelin content. Further, derived parameters can be affected by various physiological aspects including iron content, fiber fanning or crossing, microstructural complexity, or cell membrane permeability (18,19).

To overcome these limitations, advanced MRI methods have been developed based on multicomponent relaxometry that provide much greater sensitivity and specificity in noninvasive MRI myelin mapping (20,21). In multicomponent relaxometry, the magnetic resonance signal is separated into 2 pools of water, corresponding to the intra/extracellular water pool and the water trapped between the myelin sheaths calculated as the myelin water fraction (MWF), which has been shown to represent a direct measure of myelin content (20,21). This developing methodology allows for substantially more accurate investigation of the role of myelin degeneration in the pathogenesis of neurodegenerative diseases (20). Using MWF imaging, Boa Sorte Silva et al. found significant associations between lower MWF and higher gait variability in several cerebral structures including the cingulum, superior longitudinal fasciculus, posterior corona radiata, and the body of the corpus callosum among individuals with MCI and cerebral small vessel disease (22). However, to the best of our knowledge, no MRI studies have employed multicomponent relaxometry to explore the specific relationship between myelin content and gait speed in cognitively unimpaired individuals. Indeed, breakdown of myelin and oligodendrocytes, the specialized glial cells responsible for myelin synthesis in axons, has been shown to not only contribute to the development of numerous demyelinating diseases (23), but also to other neurodegenerative and psychiatric conditions, including MCI and dementias (24,25), with concomitant cognitive and motor deficits. Therefore, we hypothesize that lower MWF would be associated with lower gait speed.

Accordingly, we investigated the association between usual or rapid gait speed and regional myelin content in a large cohort of cognitively unimpaired adults (N = 118), ranging in age from 22 to 94 years. The inclusion of subjects that span a wide age range ensures the incorporation of a large range of myelin content and gait speeds, permitting a robust correlation analysis across adulthood. Myelin content was measured using the Bayesian Monte Carlo (BMC)–mcDESPOT-based MWF method (26), while gait speeds were measured using our established protocol (27). We also measured longitudinal and transverse relaxation rates (R_1 and R_2), which are sensitive measures to myelin content. Indeed, R_1 and R_2 depend on water mobility as well as macromolecular tissue composition, especially lipids and iron, which form the main constituents of myelin (19). These metrics are derived, assuming a monocomponent system, from the same MRI data used in the BMC–mcDESPOT modeling without extra scan time. They are expected to exhibit great sensitivity to myelin content given the very short echo times used in the corresponding MRI sequences, which allows a great detection of the signal originating from the rapidly relaxing water pool, which corresponds to the myelin water pool. Thus, the primary objective of this study is to characterize the regional associations between cerebral myelination and gait speeds in cognitively unimpaired adults.

Materials and Methods

Study Cohort

Participants were drawn from 2 ongoing healthy aging cohorts at the National Institute on Aging (NIA), the Baltimore Longitudinal Study of Aging (BLSA) and the Genetic and Epigenetic Signatures of Translational Aging Laboratory Testing (GESTALT). The study populations, experimental design, and measurement protocols of the BLSA have been previously reported (28,29). The BLSA is a longitudinal cohort study funded and conducted by the NIA Intramural Research Program (IRP). Established in 1958, the BLSA enrolls community-dwelling adults with no major chronic conditions or functional impairments (29). The GESTALT study is also a study of healthy volunteers, initiated in 2015, and funded and conducted by the NIA IRP. The goal of the BLSA and GESTALT studies is to evaluate multiple biomarkers related to aging. We note that the inclusion and exclusion criteria for these 2 studies are essentially identical. Participants underwent testing at the NIA's clinical research unit and were excluded if they had metallic implants, neurologic or medical disorders. At the time of enrollment in our MRI protocol, participants were free of central nervous system disease (dementia, stroke, bipolar illness, epilepsy), severe cardiac disease, severe pulmonary disease, and metastatic cancer. Participants underwent a Mini-Mental State Examination (MMSE). Clinical and neuropsychological data from participants were reviewed at a consensus conference if they screened positive on the Blessed Information–Memory–Concentration (BIMC) score (score ≥4), if their Clinical Dementia Rating (CDR) score was ≥0.5 using subject or informant report, or if concerns were raised about their cognitive status. The CDR was administered to positron emission tomography (PET) neuroimaging study and autopsy study participants at each visit and to the remaining participants if they scored 4 or more BIMC errors. Diagnoses of dementia and AD were based on Diagnostic and Statistical Manual of Mental Disorders and the National Institute of Neurological and Communication Disorders and Stroke—Alzheimer's Disease and Related Disorders Association criteria, respectively. MCI was based on the Petersen criteria and diagnosed when (1) cognitive impairment was evident for a single domain (typically memory) or (2) cognitive impairment in multiple domains occurred without significant functional loss in activities of daily living. Cognitively normal status was based on either (i) a CDR of zero and/or ≤3 errors on the BIMC Test, and therefore the participant did not meet the criteria for consensus conference; or (ii) the participant was determined to be cognitively normal based on a thorough review of clinical and neuropsychological data. Experimental procedures were performed in compliance with our local Institutional Review Board,

and participants provided written informed consent in accordance with the Declaration of Helsinki prior to investigation.

Data Acquisition

Each participant underwent our BMC–mcDESPOT protocol for MWF, R_1, and R_2 mapping (26). This imaging protocol consists of 3D spoiled gradient recalled echo (SPGR) images acquired with flip angles (FAs) of [2 4 6 8 10 12 14 16 18 20]°, echo time (TE) of 1.37 ms, repetition time (TR) of 5 ms, and acquisition time of ~5 minutes, as well as 3D balanced steady-state free precession (bSSFP) images acquired with FAs of [2 4 7 11 16 24 32 40 50 60]°, TE of 2.8 ms, TR of 5.8 ms, and acquisition time of ~6 minutes. The bSSFP images were acquired with radiofrequency (RF) excitation pulse phase increments of 0 or 180° to account for the off-resonance effects (30), with a total scan time of ~12 minutes. All SPGR and bSSFP images were acquired with an acquisition matrix of 150 × 130 × 94 and a voxel size of 1.6 mm × 1.6 mm × 1.6 mm. To correct for excitation RF inhomogeneity (31), we used the double-angle method (DAM), which consisted of acquiring 2 fast spin-echo images with FAs of 45° and 90°, TE of 102 ms, TR of 3 000 ms, acquisition voxel size of 2.6 mm × 2.6 mm × 4 mm, and acquisition time of ~4 minutes. All images were acquired with field-of-view of 240 mm × 208 mm × 150 mm, SENSitivity Encoding factor of 2, and reconstructed to a voxel size of 1 mm × 1 mm × 1 mm. The total acquisition time was ~21 minutes. MRI scans were performed on a 3-T whole-body Philips MRI system (Achieva, Best, The Netherlands) using the internal quadrature body coil for transmission and an 8-channel phased-array head coil for reception. We emphasize that all MRI studies and ancillary measurements were performed with the same MRI system, with the same pulse sequences, and at the same facility for both BLSA and GESTALT participants.

Data Processing

For each participant, using the FMRIB's Linear Image Registration Tool analysis as implemented in the FSL software (32), all SPGR, bSSFP, and DAM images were linearly registered to the SPGR image obtained at FA of 8° and the respective derived transformation matrices were then applied to the original SPGR, bSSFP, or DAM images. A whole-brain MWF map was then generated using BMC–mcDESPOT from these co-registered SPGR, bSSFP, and DAM data sets (26,33). BMC–mcDESPOT assumes a 2-relaxation time component system consisting of a short T_2 component, attributed to myelin water, and a long T_2 component, attributed to intra and extracellular waters. We used the signal model explicitly accounting for nonzero TE (34). This emerging method offers rapid and reliable whole-brain MWF maps (26,33–35). A whole-brain R_1 map was generated from the co-registered SPGR and DAM data sets using DESPOT1 and assuming a single component longitudinal relaxation component, and a whole-brain R_2 map was generated from the co-registered bSSFP and DAM data sets using DESPOT2, also assuming a single component (36). R_1 and R_2 values depend on both water mobility and macromolecular tissue composition, including local lipid and iron content, and thus are expected to be directly associated with a number of microstructural features of brain tissue, including myelin content.

Further, using FSL software (32), the averaged SPGR image over FAs underwent nonlinear registration to the Montreal Neurological Institute (MNI) standard space, and the computed transformation matrix was then applied to the corresponding MWF, R_1, and R_2 maps. An example of the quality of the parameter maps' registration is shown in Supplementary Figure 1A. Twenty-one white matter regions of interest (ROIs) were defined from the MNI structural atlas (Supplementary Figure 1B). These encompassed the whole brain, the frontal, parietal, temporal, and occipital lobes, cerebellum, the body, genu, and splenium of the corpus callosum, internal capsule, cerebral peduncle, anterior and posterior corona radiata, anterior and posterior thalamic radiation, superior and inferior fronto-occipital fasciculus, superior and inferior longitudinal fasciculus, and forceps major and minor. ROIs were defined in the MNI space and have been eroded to reduce partial volume effects and imperfect image registration using a kernel box of 2 voxels × 2 voxels × 2 voxels with the FSL tool *fslmaths*. Within each ROI, the mean MWF, R_1, and R_2 values were calculated.

Usual and Rapid Gait Speed Measurement

Usual gait speed (UGS; unit, m/s) was assessed by asking participants to walk at their "usual, comfortable pace" over a 6-m course in an uncarpeted corridor. Participants stood with their feet behind a taped starting line. After a command of "Go", timing was initiated with the first foot-fall over the starting line and stopped after the first foot-fall over the finish line. Similarly, rapid gait speed (RGS; unit, m/s) was measured after instructing the participants to walk as quickly as possible, without running (27). Of note, gait speeds were measured after 2 trials, and the fastest value measure was used in the subsequent analyses. We note that all MRI and gait speed measurements were performed at the same facility and within the same day.

Statistical Analysis

To investigate the effect of MWF, R_1, or R_2 on RGS or UGS, a multiple linear regression analysis was performed using the mean RGS or UGS value as the dependent variable, and age, sex, race, MMSE, body mass index (BMI), and MWF, R_1, or R_2 values within each ROI as independent variables. The continuous variables were Z-scored by subtracting the mean value calculated across participants from each measured value and dividing by the standard deviation value. The initial model incorporated an interaction term between age and MWF, R_1, or R_2 but was removed as it was found not to be significant in any of the ROIs investigated. The resulting parsimonious model was then constructed without this interaction term. The final regression model is given by:

$$\begin{aligned} gait\ speed\ (m/s) \ \sim\ & \beta_o + \beta_{age} \times age + \beta_{sex} \\ & \times sex + \beta_{race} \times race \ + \ \beta_{BMI} \times BMI \\ & + \beta_{MMSE} \times \ MMSE + \beta_{MRI} \times MRI \end{aligned}$$

where MRI corresponds to MWF, R_1, or R_2. The threshold for statistical significance was taken as $p < .05$, while close-to-significance was taken as $p < .1$, after correction for multiple ROI comparisons using the false discovery rate (FDR) method (37,38). All analyses were run using MATLAB software (MathWorks, Natick, MA).

Results

Cohort's Characteristics

Demographic characteristics of the participants are shown in Table 1. The age and sex distribution of the participants are provided in Supplementary Figure 2. After removal of 22 participants' data sets with either missing data, severe motion artifacts on the MR images assessed using visual inspection, or from participants with cognitive impairments, the final cohort consisted of 118 cognitively unimpaired

Table 1. Demographic Characteristics of Study Participants

Total sample	*N* = 118
Age (years), mean ± *SD (min–max)*	55.4 ± 20.4 *(22–94)*
Sex	
Male, *N* (%)	64 *(54.2%)*
Female, *N* (%)	54 *(45.8%)*
Race	
White, *N* (%)	82 *(69.4%)*
Black, *N* (%)	24 *(20.3%)*
Other, *N* (%)	12 *(10.2%)*
MMSE, mean ± *SD (min–max)*	28.8 ± 1.4 *(25–30)*
BMI (kg/m^2), mean ± *SD (min–max)*	25.8 ± 3.6 *(18.3–35.8)*
RGS (m/s), mean ± *SD (min–max)*	1.85 ± 0.33 *(0.92–2.67)*
UGS (m/s), mean ± *SD (min–max)*	1.24 ± 0.22 *(0.68–1.81)*

Notes: BMI = body mass index; max = maximum; min = minimum; MMSE = Mini-Mental State Examination; RGS = rapid gait speed; UGS = usual gait speed; *SD* = standard deviation. Values are given as either the mean ± standard deviation (range), or the *N* (%).

volunteers (mean ± standard deviation MMSE = 28.8 ± 1.4) ranging in age from 22 to 94 years (55.4 ± 20.4 years). Of this final cohort, 54 (45.8%) were women, while 82 (69.4%) were White and 24 (20.3%) were Black. The mean ± standard deviation values of BMI were 25.8 ± 3.6. The mean ± standard deviation values of RGS and UGS were 1.85 ± 0.33 m/s and 1.24 ± 0.22 m/s, respectively.

Associations Between Gait Speeds and Cerebral Microstructure

Figure 1 shows MWF, R_1, and R_2 MR parameter maps of participants with either higher or lower RGS or UGS values within a limited age range between 52 and 70 years to mitigate the effect of age. Higher RGS or UGS correspond to values above the mean values calculated across this restricted age-range group, while lower RGS or UGS correspond to values below or equal to the mean value. This limited age range minimizes the potential effect of age on derived MR parameter maps for this qualitative analysis; statistical quantification of the effect of age as a covariate will be presented below. Visual inspection indicates that, overall, participants with lower RGS or UGS values exhibit smaller regional MWF, R_1, and R_2 values, and, conversely, participants with higher regional RGS or UGS values exhibit the highest regional MWF, R_1, and R_2 values. In other words, higher myelin content is associated with higher gait speeds. These qualitative results suggest a potential strong association between RGS or UGS and myelin content.

Figure 2 shows an example of plots of the associations between RGS or UGS, and MWF, R_1, or R_2, derived from the whole-brain white matter ROI, from the multiple regressions analysis, after adjusting for age, sex, race, MMSE, and BMI. In agreement with the visual inspection of Figure 1, there are positive correlations between all 3 MRI measures investigated and RGS or UGS, with lower MWF, R_1, and R_2 values corresponding to lower RGS and UGS values. We found that, except for the body and genu of the corpus callosum and cerebral peduncles for MWF and R_2, the associations between RGS and MWF, R_1, and R_2 were statistically significant ($p < .05$) in most ROIs investigated after FDR correction (Table 2). We also note that, overall, the frontal and parietal lobes, the splenium and the main anterior or superior subcortical white matter tracts—namely, the superior fronto-occipital fasciculus, superior longitudinal fasciculus, and anterior corona radiata—exhibited the steepest slopes between RGS and MWF, R_1, and R_2, indicating stronger correlations.

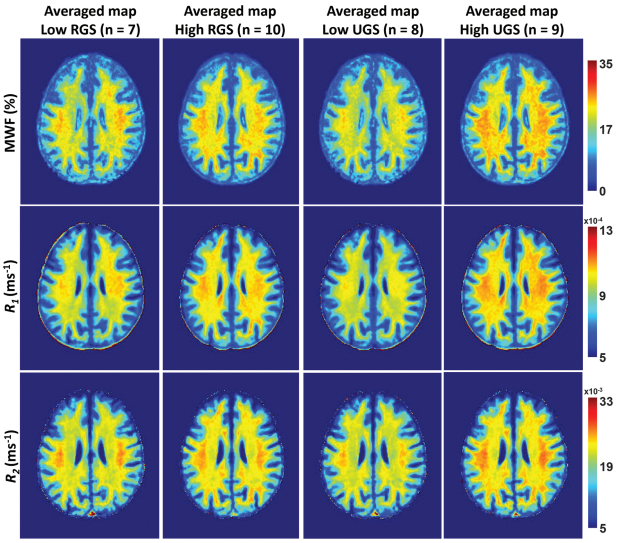

Figure 1. MWF, R_1, and R_2 parameter maps averaged across participants drawn from a limited age range (52–70 years) with either higher or lower RGS or UGS values. R_1 = longitudinal relaxation rate; R_2 = transverse relaxation rate. MWF = myelin water fraction; RGS = rapid gait speed; UGS = usual gait speed. Results are shown for a representative imaging slice. Visual inspection indicates that, overall, participants with lower RGS or UGS values exhibit smaller regional MWF, R_1, and R_2 values, while participants with higher RGS or UGS values exhibit higher regional MWF, R_1, and R_2 values.

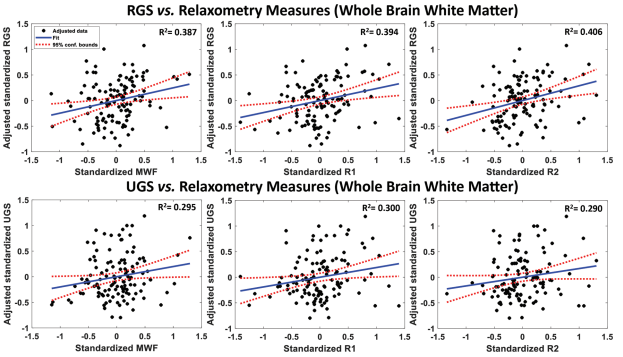

Figure 2. Regression plots of the standardized RGS (top) and UGS (bottom) values as a function of standardized MWF (left panel), R_1 (middle panel), or R_2 (right panel) values within the whole-brain white matter. R_1 = longitudinal relaxation rate; R_2 = transverse relaxation rate; MWF = myelin water fraction; RGS = rapid gait speed; UGS = usual gait speed. Values are adjusted for sex, race, MMSE, and body mass index. For each plot, the best-fit line (blue solid line) and confidence intervals (red dashed lines) are displayed. The adjusted response function describes the relationship between the indicated dependent variable and MWF, R_1, or R_2 with the other predictors averaged out by averaging the fitted values over the data used in the fit. There are positive correlations between all magnetic resonance parameters and RGS or UGS.

Furthermore, as expected, the correlation between age and RGS was statistically significant and exhibited negative slopes across all ROIs investigated (Table 2), with lower values of RGS in the older participants. We note that, for all ROIs, the effect of aging on RGS was stronger than the effect of MWF, R_1, or R_2 (Table 2). Additionally, we note that there were no significant associations between RGS and sex, race, MMSE, or BMI in any of the ROIs evaluated (Supplementary Tables 1–3).

Table 2. Regression Coefficient (standard error) and *p* Values (after FDR correction) of MWF, R_1, or R_2, and Age With Respect to RGS for Each of the 21 WM ROIs Investigated

	MWF		R_1		R_2	
ROIs	RGS	Age	RGS	Age	RGS	Age
WB	0.25 *(0.09)*, **.030**	−0.45 *(0.10)*, **<.001**	0.30 *(0.08)*, **.004**	−0.48 *(0.09)*, **<.001**	0.25 *(0.09)*, **.024**	−0.43 *(0.10)*, **<.001**
FL	0.28 *(0.10)*, **.030**	−0.43 *(0.10)*, **<.001**	0.29 *(0.08)*, **.004**	−0.48 *(0.09)*, **<.001**	0.26 *(0.10)*, **.027**	−0.42 *(0.10)*, **<.001**
OL	0.15 *(0.08)*, .086	−0.53 *(0.09)*, **<.001**	0.23 *(0.08)*, **.005**	−0.53 *(0.09)*, **<.001**	0.18 *(0.09)*, .054	−0.49 *(0.09)*, **<.001**
PL	0.23 *(0.09)*, **.030**	−0.46 *(0.10)*, **<.001**	0.24 *(0.08)*, **.007**	−0.50 *(0.09)*, **<.001**	0.22 *(0.10)*, **.048**	−0.45 *(0.10)*, **<.001**
TL	0.19 *(0.09)*, **.042**	−0.50 *(0.09)*, **<.001**	0.25 *(0.08)*, **.005**	−0.51 *(0.09)*, **<.001**	0.22 *(0.09)*, **.029**	−0.46 *(0.10)*, **<.001**
CRB	0.18 *(0.08)*, **.042**	−0.51 *(0.09)*, **<.001**	0.23 *(0.08)*, **.005**	−0.54 *(0.08)*, **<.001**	0.18 *(0.08)*, .054	−0.50 *(0.09)*, **<.001**
BCC	0.15 *(0.09)*, .125	−0.50 *(0.10)*, **<.001**	0.29 *(0.09)*, **.004**	−0.45 *(0.09)*, **<.001**	0.12 *(0.09)*, .199	−0.51 *(0.10)*, **<.001**
GCC	0.15 *(0.09)*, .110	−0.50 *(0.10)*, **<.001**	0.23 *(0.09)*, **.011**	−0.47 *(0.09)*, **<.001**	0.13 *(0.10)*, .199	−0.50 *(0.10)*, **<.001**
SCC	0.25 *(0.09)*, **.030**	−0.47 *(0.09)*, **<.001**	0.28 *(0.08)*, **.004**	−0.50 *(0.09)*, **<.001**	0.25 *(0.09)*, **.023**	−0.46 *(0.09)*, **<.001**
IC	0.23 *(0.09)*, **.030**	−0.46 *(0.10)*, **<.001**	0.25 *(0.08)*, **.004**	−0.49 *(0.09)*, **<.001**	0.21 *(0.09)*, **.047**	−0.46 *(0.10)*, **<.001**
CP	0.12 *(0.08)*, .134	−0.55 *(0.09)*, **<.001**	0.16 *(0.08)*, **.047**	−0.56 *(0.09)*, **<.001**	0.11 *(0.08)*, .199	−0.54 *(0.09)*, **<.001**
ACR	0.29 *(0.09)*, **.022**	−0.43 *(0.10)*, **<.001**	0.30 *(0.08)*, **.004**	−0.46 *(0.09)*, **<.001**	0.31 *(0.09)*, **.022**	−0.41 *(0.10)*, **<.001**
PCR	0.24 *(0.09)*, **.030**	−0.45 *(0.10)*, **<.001**	0.28 *(0.09)*, **.004**	−0.47 *(0.09)*, **<.001**	0.20 *(0.10)*, .057	−0.47 *(0.10)*, **<.001**
AThR	0.20 *(0.09)*, **.042**	−0.49 *(0.09)*, **<.001**	0.26 *(0.08)*, **.005**	−0.49 *(0.09)*, **<.001**	0.16 *(0.09)*, .100	−0.51 *(0.10)*, **<.001**
PThR	0.21 *(0.09)*, **.042**	−0.46 *(0.10)*, **<.001**	0.26 *(0.09)*, **.005**	−0.46 *(0.09)*, **<.001**	0.25 *(0.09)*, **.024**	−0.44 *(0.10)*, **<.001**
SFOF	0.34 *(0.09)*, **.010**	−0.39 *(0.10)*, **<.001**	0.25 *(0.08)*, **.005**	−0.48 *(0.09)*, **<.001**	0.31 *(0.10)*, **.023**	−0.39 *(0.10)*, **<.001**
IFOF	0.16 *(0.09)*, .095	−0.50 *(0.10)*, **<.001**	0.24 *(0.08)*, **.004**	−0.50 *(0.09)*, **<.001**	0.17 *(0.09)*, .072	−0.49 *(0.10)*, **<.001**
SLF	0.25 *(0.09)*, **.030**	−0.46 *(0.10)*, **<.001**	0.28 *(0.08)*, **.004**	−0.48 *(0.09)*, **<.001**	0.27 *(0.09)*, **.023**	−0.43 *(0.10)*, **<.001**
ILF	0.16 *(0.09)*, .095	−0.51 *(0.09)*, **<.001**	0.20 *(0.09)*, **.019**	−0.52 *(0.09)*, **<.001**	0.21 *(0.09)*, **.043**	−0.47 *(0.10)*, **<.001**
FMAJ	0.22 *(0.09)*, **.030**	−0.48 *(0.09)*, **<.001**	0.27 *(0.08)*, **.004**	−0.49 *(0.09)*, **<.001**	0.26 *(0.09)*, **.023**	−0.45 *(0.09)*, **<.001**
FMIN	0.24 *(0.10)*, **.030**	−0.44 *(0.10)*, **<.001**	0.29 *(0.09)*, **.004**	−0.47 *(0.09)*, **<.001**	0.19 *(0.10)*, .066	−0.46 *(0.10)*, **<.001**

Notes: ACR = anterior corona radiata; AThR = anterior thalamic radiation; BCC = body of corpus callosum; CP = cerebral peduncle; CRB = cerebellum; FDR = false discovery rate; FL = frontal lobe; FMAJ = forceps major; FMIN = forceps minor; GCC = genu of corpus callosum; IC = internal capsule; IFOF = inferior fronto-occipital fasciculus; ILF = inferior longitudinal fasciculus; MWF = myelin water fraction; OL = occipital lobe; PCR = posterior corona radiata; PL = parietal lobe; PThR = posterior thalamic radiation; R_1 = longitudinal relaxation rate; R_2 = transverse relaxation rate; RGS = rapid gait speed; ROI = region-of-interest; SCC = splenium of corpus callosum; SFOF = superior fronto-occipital fasciculus; SLF = superior longitudinal fasciculus; TL = temporal lobe; WB = whole brain; WM = white matter. The multiple regression model used is given by: RGS ~ $\beta_0 + \beta_{age} \times age + \beta_{MRI} \times MRI + \beta_{BMI} \times BMI + \beta_{sex} \times sex + \beta_{race} \times race + \beta_{MMSE} \times MMSE$, where MRI corresponds to MWF, R_1, or R_2. Bold indicates statistical significance ($p < .05$) after FDR correction. Italic indicates SE. We note that the full results of all covariates incorporated in the multiple regression model are shown in Supplementary Tables 1–3.

Table 3. Regression Coefficient (standard error) and *p* Value (after FDR correction) of MWF, R_1, or R_2, and Age With Respect to UGS for Each of the 21 WM ROIs Investigated

	MWF		R_1		R_2	
ROIs	UGS	Age	UGS	Age	UGS	Age
WB	0.18 *(0.10)*, .167	−0.30 *(0.10)*, **.005**	0.17 *(0.09)*, .092	−0.34 *(0.10)*, **.001**	0.23 *(0.10)*, .074	−0.26 *(0.11)*, **.019**
FL	0.21 *(0.10)*, .167	−0.28 *(0.11)*, **.011**	0.16 *(0.09)*, .098	−0.34 *(0.10)*, **.001**	0.26 *(0.10)*, .062	−0.24 *(0.11)*, **.038**
OL	0.10 *(0.09)*, .279	−0.36 *(0.10)*, **.003**	0.15 *(0.09)*, .094	−0.36 *(0.09)*, **.001**	0.16 *(0.09)*, .121	−0.32 *(0.10)*, **.009**
PL	0.15 *(0.10)*, .219	−0.32 *(0.10)*, **.004**	0.12 *(0.09)*, .202	−0.36 *(0.10)*, **.001**	0.18 *(0.10)*, .121	−0.29 *(0.11)*, **.014**
TL	0.12 *(0.09)*, .231	−0.34 *(0.10)*, **.004**	0.19 *(0.09)*, .091	−0.34 *(0.09)*, **.001**	0.18 *(0.09)*, .101	−0.30 *(0.10)*, **.010**
CRB	0.19 *(0.09)*, .167	−0.33 *(0.09)*, **.004**	0.19 *(0.08)*, .091	−0.37 *(0.09)*, **.001**	0.20 *(0.09)*, .074	−0.31 *(0.10)*, **.009**
BCC	0.13 *(0.10)*, .231	−0.32 *(0.11)*, **.005**	0.19 *(0.10)*, .091	−0.31 *(0.10)*, **.003**	0.16 *(0.10)*, .121	−0.31 *(0.11)*, **.010**
GCC	0.18 *(0.10)*, .167	−0.30 *(0.10)*, **.005**	0.18 *(0.10)*, .091	−0.31 *(0.10)*, **.003**	0.17 *(0.10)*, .121	−0.30 *(0.11)*, **.013**
SCC	0.19 *(0.10)*, .167	−0.31 *(0.10)*, **.004**	0.23 *(0.09)*, .091	−0.33 *(0.09)*, **.001**	0.27 *(0.09)*, .053	−0.27 *(0.10)*, **.013**
IC	0.14 *(0.10)*, .227	−0.33 *(0.10)*, **.004**	0.19 *(0.09)*, .091	−0.33 *(0.09)*, **.001**	0.13 *(0.10)*, .213	−0.33 *(0.11)*, **.009**
CP	0.15 *(0.08)*, .167	−0.36 *(0.09)*, **.003**	0.19 *(0.08)*, .091	−0.38 *(0.09)*, **.001**	0.19 *(0.09)*, .074	−0.33 *(0.09)*, **.009**
ACR	0.24 *(0.10)*, .167	−0.27 *(0.10)*, **.011**	0.22 *(0.09)*, .091	−0.31 *(0.10)*, **.002**	0.32 *(0.10)*, .023	−0.22 *(0.10)*, **.038**
PCR	0.17 *(0.10)*, .172	−0.31 *(0.11)*, **.005**	0.17 *(0.09)*, .092	−0.33 *(0.10)*, **.001**	0.16 *(0.10)*, .124	−0.31 *(0.11)*, **.010**
AThR	0.16 *(0.10)*, .172	−0.32 *(0.10)*, **.004**	0.19 *(0.09)*, .091	−0.33 *(0.10)*, **.001**	0.12 *(0.10)*, .213	−0.34 *(0.10)*, **.009**
PThR	0.16 *(0.10)*, .197	−0.31 *(0.11)*, **.005**	0.22 *(0.09)*, .091	−0.30 *(0.10)*, **.003**	0.20 *(0.10)*, .091	−0.28 *(0.11)*, **.013**
SFOF	0.24 *(0.10)*, .167	−0.26 *(0.11)*, **.014**	0.18 *(0.09)*, .091	−0.33 *(0.10)*, **.001**	0.27 *(0.11)*, .062	−0.23 *(0.11)*, **.038**
IFOF	0.12 *(0.10)*, .231	−0.34 *(0.10)*, **.004**	0.17 *(0.09)*, .091	−0.34 *(0.10)*, **.001**	0.16 *(0.10)*, .121	−0.31 *(0.10)*, **.009**
SLF	0.12 *(0.10)*, .249	−0.34 *(0.10)*, **.004**	0.16 *(0.09)*, .098	−0.34 *(0.10)*, **.001**	0.21 *(0.10)*, .082	−0.28 *(0.11)*, **.013**
ILF	0.11 *(0.09)*, .266	−0.35 *(0.10)*, **.004**	0.16 *(0.09)*, .092	−0.35 *(0.09)*, **.001**	0.16 *(0.09)*, .121	−0.32 *(0.10)*, **.009**
FMAJ	0.16 *(0.09)*, .167	−0.33 *(0.10)*, **.004**	0.21 *(0.09)*, .091	−0.33 *(0.09)*, **.001**	0.25 *(0.09)*, .060	−0.27 *(0.10)*, **.013**
FMIN	0.19 *(0.10)*, .167	−0.29 *(0.11)*, **.008**	0.17 *(0.09)*, .092	−0.33 *(0.10)*, **.001**	0.19 *(0.10)*, .111	−0.28 *(0.11)*, **.014**

Notes: ACR = anterior corona radiata; AThR = anterior thalamic radiation; BCC = body of corpus callosum; CP = cerebral peduncle; CRB = cerebellum; FDR = false discovery rate; FL = frontal lobe; FMAJ = forceps major; FMIN = forceps minor; GCC = genu of corpus callosum; IC = internal capsule; IFOF = inferior fronto-occipital fasciculus; ILF = inferior longitudinal fasciculus; MWF = myelin water fraction; OL = occipital lobe; PCR = posterior corona radiata; PL = parietal lobe; PThR = posterior thalamic radiation; R_1 = longitudinal relaxation rate; R_2 = transverse relaxation rate; ROI = region-of-interest; SCC = splenium of corpus callosum; SFOF = superior fronto-occipital fasciculus; SLF = superior longitudinal fasciculus; TL = temporal lobe; UGS = usual gait speed; WB = whole brain; WM = white matter. The multiple regression model used is given by: UGS ~ $\beta_0 + \beta_{age} \times$ age + $\beta_{MRI} \times$ MRI + $\beta_{BMI} \times$ BMI + $\beta_{sex} \times$ sex + $\beta_{race} \times$ race + $\beta_{MMSE} \times$ MMSE, where MRI corresponds to MWF, R_1, or R_2. Bold indicates statistical significance ($p < .05$) after FDR correction. Italic indicates SE. We note that the full results of all covariates incorporated in the multiple regression model are shown in Supplementary Tables 4–6.

In contrast, the association between UGS and MWF was not significant in any of the ROIs investigated, after FDR correction (Table 3). However, several ROIs exhibited significance ($p < .05$) before FDR correction, including the cerebellum, splenium, anterior corona radiata, and superior fronto-occipital fasciculus. Similarly, the association between UGS and R_1 was close-to-significant in all ROIs investigated, except the parietal lobes ROI after FDR correction. Here again, the steepest slopes were, overall, seen in the frontal lobes, superior fronto-occipital fasciculus, and anterior corona radiata fiber tracts. We note that the effect of MWF, R_1, and R_2 was, overall, much stronger on RGS than UGS (Tables 2 and 3). Finally, as expected, the effect of age on UGS was significant in all ROIs investigated, with age exhibiting a much stronger effect on UGS as compared to MWF, R_1, or R_2 (Table 3). We also note that while the effects of sex, race, and MMSE were not significant, the effect of BMI on UGS was significant in all ROIs investigated (Supplementary Tables 4–6).

Discussion

In this cross-sectional study, using multicomponent MR relaxometry for both direct and indirect measurements of myelin content, we demonstrate that lower gait speeds were associated with lower myelin content, as measured by the MWF and relaxation rates. These regional associations were observed in a relatively large cohort of well-characterized, cognitively unimpaired, adults spanning a wide age range. These findings provide further evidence of the association between physical function, quantified with gait speeds, and neurodegeneration in white matter, measured using a more specific (MWF) and less specific (R_1, R_2) MRI measures of myelin content. Moreover, to our knowledge, this is the first investigation to indicate that RGS is a more robust indicator of demyelination as compared to UGS; this may serve as an early indicator of neurodegeneration and allow for early interventions for MCI and AD. While our results do not prove causality, they are consistent with the notion that lower myelin content may contribute to gait speed impairments in normative aging, thus linking white matter myelin integrity and motor function.

We found significant positive correlations in most critical white matter brain regions between RGS and MWF values, even after FDR correction and adjustment for age, sex, race, MMSE, and BMI (Figure 2; Table 2). These regional associations were also markedly significant for R_1. Indeed, R_1 depends on water mobility as well as macromolecular tissue composition, especially lipids, which form the main constituent of myelin. However, unlike MWF, the associations between RGS and R_1 were significant in all ROIs studied. There are several considerations that could explain these observations. First, R_1 determination relies on a simple monocomponent signal model so that a precise and accurate determination is achieved in all cerebral structures, providing high sensitivity in capturing the association between myelin content and RGS. In contrast, MWF determination relies on multicomponent analysis, which involves more complex signal modeling that inherently leads to lower accuracy and precision in derived values (39). Second, although R_1 is very sensitive to myelin content, it is also sensitive to other physiological parameters such as axonal or synaptic density. Therefore, the associations between lower R_1 and RGS may also reflect confounding effects. Indeed, our results support this notion by indicating that R_2, an MR parameter that is very sensitive to axonal density (35), is also significantly associated with RGS in several ROIs. Further analyses, including multishell diffusion imaging for the direct measurement of neurite and axonal density, may provide additional insights into this specific relationship; this work is in progress.

Interestingly, while we found significant or close-to-significant associations between all MRI metrics and RGS across almost all ROIs, we found that, overall, the frontal and parietal lobes, the splenium of the corpus callosum, and the main anterior or superior subcortical white matter tracts—namely, the superior fronto-occipital fasciculus, superior longitudinal fasciculus, and the anterior corona radiata—exhibited the steepest slopes between RGS and our relaxometry parameters (Table 2). These associations between RGS and MWF, R_1, or R_2 were weaker within the temporal and occipital lobes, the body and genu of the corpus callosum, and the main posterior and inferior subcortical white matter tracts.

Our finding of strong associations between RGS and our relaxometry parameters within the frontal and parietal lobes, splenium, superior fronto-occipital fasciculus, superior longitudinal fasciculus, and the anterior corona radiata corroborate previous structural MRI and DTI studies (9,11–17). Indeed, cognitive and motor declines share common underlying pathophysiological pathways and neural substrates (4). Despite its apparent simplicity, proper gait requires a complex interplay between sensory integration, frontal executive function and motor planning, and attention and cognitive control. It is well-established, especially in functional MRI research, that the frontal and parietal cerebral structures closely interact forming a single neural network, the fronto-parietal control network, to facilitate executive processes and direct cognitive control (40), while disruptions in fronto-parietal white matter pathways have previously been shown to be related to impaired motor and executive functions in individuals with MCI or AD (41). Additionally, several studies have shown that the anterior corona radiata and the superior fronto-occipital and longitudinal fasciculus may serve an important role in information processing, executive function, and motor control (9,15,42), which may explain their association with RGS seen here. Finally, our finding of an association within the splenium is likely due to its involvement in the integration and interhemispheric transfer of visual and somatosensory inputs between the parietal and occipital cortices (15,43), which is necessary for gait performance. Hence, our results suggest that demyelination in brain regions responsible for sensory integration, motor and executive processes, and cognitive control could play a more prominent role in RGS disturbances as compared to other brain regions.

We did not find any significant associations between UGS and MWF, and only close-to-significant associations between UGS and R_1 or R_2 in a limited number of ROIs (Table 3). These findings suggest that RGS may be a more sensitive marker of demyelination than UGS, in agreement with existing literature. For example, RGS (also referred to as fast gait speed) has been shown to be a more sensitive marker of neuromuscular function than UGS among older individuals (44). Additionally, RGS has been shown to better reveal gait deficits in individuals with neurodegenerative diseases compared to UGS (45,46). Moreover, RGS has been shown to be more robust than UGS in differentiating levels of cognition in cognitively unimpaired older adults (47), in identifying stages of cognitive decline (cognitively healthy, MCI, and dementia) (48), and in predicting accelerated cognitive decline over time (49). These findings may be due to the higher cognitive and physiological demands placed on the brain during strenuous physical activities in RGS performance compared to less challenging physical activities that require limited brain resources in UGS performance. It is possible that these higher demands placed on the brain during RGS performance necessitate greater cognitive control and neuronal activity, particularly in white

matter regions involved in frontal executive function and motor processes. Therefore, RGS performance may have clinical utility in detecting latent pathology, including myelin loss, that could facilitate diagnosis of neurodegenerative diseases.

Although our investigation examined a relatively large cohort and used advanced MRI methodology to probe myelin content, our work has certain limitations. We used cross-sectional data; longitudinal studies will be needed to determine the causality of the RGS and myelin associations observed here. Further, while the BLSA and GESTALT participants included in this study were very healthy without history of chronic diseases or hip replacements, other covariates that are not accounted for here may affect determination of gait speeds or our results, including vision or self-efficacy. Moreover, contamination due to partial volume issues may have been introduced in the calculated relaxometry metric values. To mitigate the potential effects of partial volume contamination, all ROIs were eroded followed by careful visual inspection. Nevertheless, some partial volume effects could have persisted, especially in small structures. We also note that determination of MR parameters can be biased due to several experimental and physiological factors. These include, but are not limited to, the effects of magnetization transfer between macromolecules and free water protons, exchange between water pools, *J*-coupling, off-resonance, spin-locking effects, water diffusion within different compartments, and internal gradients. Further technical developments are thus needed to improve the accuracy of MRI studies of myelin content. Finally, a histological validation of the MWF measured using BMC–mcDESPOT has not previously been performed and is still needed to establish the extent of specificity of this metric to myelin content. This work is underway.

Conclusion

Our study provides new insights into the importance of myelin on physical functioning indicating that loss of cerebral myelination is associated with age-related gait impairments among cognitively healthy individuals. This work forms the basis for further investigations to elucidate the specific relationship between gait speeds and myelination in cognitive impairments, including in AD.

Supplementary Material

Supplementary data are available at *The Journals of Gerontology, Series A: Biological Sciences and Medical Sciences* online.

Funding

This work was supported by the Intramural Research Program of the National Institute on Aging of the National Institutes of Health.

Conflict of Interest

None declared.

References

1. Ferrucci L, Bandinelli S, Benvenuti E, et al. Subsystems contributing to the decline in ability to walk: bridging the gap between epidemiology and geriatric practice in the InCHIANTI study. *J Am Geriatr Soc*. 2000;48(12):1618–1625. doi:10.1111/j.1532-5415.2000.tb03873.x
2. Studenski S. Bradypedia: is gait speed ready for clinical use? *J Nutr Health Aging*. 2009;13(10):878–880. doi:10.1007/s12603-009-0245-0
3. Studenski S, Perera S, Patel K, et al. Gait speed and survival in older adults. *JAMA*. 2011;305(1):50–58. doi:10.1001/jama.2010.1923
4. Grande G, Triolo F, Nuara A, Welmer AK, Fratiglioni L, Vetrano DL. Measuring gait speed to better identify prodromal dementia. *Exp Gerontol*. 2019;124:110625. doi:10.1016/j.exger.2019.05.014
5. Pieruccini-Faria F, Black SE, Masellis M, et al. Gait variability across neurodegenerative and cognitive disorders: results from the Canadian Consortium of Neurodegeneration in Aging (CCNA) and the Gait and Brain Study. *Alzheimers Dement*. 2021;17(8):1317–1328. doi:10.1002/alz.12298
6. Buracchio T, Dodge HH, Howieson D, Wasserman D, Kaye J. The trajectory of gait speed preceding mild cognitive impairment. *Arch Neurol*. 2010;67(8):980–986. doi:10.1001/archneurol.2010.159
7. Skillback T, Blennow K, Zetterberg H, et al. Slowing gait speed precedes cognitive decline by several years. *Alzheimers Dement*. 2022;18(9):1667–1676. doi:10.1002/alz.12537
8. Rosano C, Bennett DA, Newman AB, et al. Patterns of focal gray matter atrophy are associated with bradykinesia and gait disturbances in older adults. *J Gerontol A Biol Sci Med Sci*. 2012;67(9):957–962. doi:10.1093/gerona/glr262
9. Rosario BL, Rosso AL, Aizenstein HJ, et al.; Health ABC Study. Cerebral white matter and slow gait: contribution of hyperintensities and normal-appearing parenchyma. *J Gerontol A Biol Sci Med Sci*. 2016;71(7):968–973. doi:10.1093/gerona/glv224
10. Tian Q, Bair WN, Resnick SM, Bilgel M, Wong DF, Studenski SA. Beta-amyloid deposition is associated with gait variability in usual aging. *Gait Posture*. 2018;61:346–352. doi:10.1016/j.gaitpost.2018.02.002
11. Snir JA, Bartha R, Montero-Odasso M. White matter integrity is associated with gait impairment and falls in mild cognitive impairment. Results from the Gait and Brain Study. *Neuroimage Clin*. 2019;24:101975. doi:10.1016/j.nicl.2019.101975
12. Bruijn SM, Van Impe A, Duysens J, Swinnen SP. White matter microstructural organization and gait stability in older adults. *Front Aging Neurosci*. 2014;6:104. doi:10.3389/fnagi.2014.00104
13. Tian Q, Williams OA, Landman BA, Resnick SM, Ferrucci L. Microstructural neuroimaging of frailty in cognitively normal older adults. *Front Med (Lausanne)*. 2020;7:546344. doi:10.3389/fmed.2020.546344
14. Ducca EL, Gomez GT, Palta P, et al. Physical frailty and brain white matter abnormalities: the ARIC study. *J Gerontol A Biol Sci Med Sci*. 2023;78(2):357–364. doi:10.1093/gerona/glac111
15. Tian Q, Ferrucci L, Resnick SM, et al. The effect of age and microstructural white matter integrity on lap time variation and fast-paced walking speed. *Brain Imaging Behav*. 2016;10(3):697–706. doi:10.1007/s11682-015-9449-6
16. Boa Sorte Silva NC, Dao E, Hsu CL, et al. Myelin and physical activity in older adults with cerebral small vessel disease and mild cognitive impairment. *J Gerontol A Biol Sci Med Sci*. 2023;78(3):545–553. doi:10.1093/gerona/glac149
17. Tian Q, Schrack JA, Landman BA, Resnick SM, Ferrucci L. Longitudinal associations of absolute versus relative moderate-to-vigorous physical activity with brain microstructural decline in aging. *Neurobiol Aging*. 2022;116:25–31. doi:10.1016/j.neurobiolaging.2022.04.007
18. Mori S, Zhang J. Principles of diffusion tensor imaging and its applications to basic neuroscience research. *Neuron*. 2006;51(5):527–539. doi:10.1016/j.neuron.2006.08.012
19. Deoni SC. Quantitative relaxometry of the brain. *Top Magn Reson Imaging*. 2010;21(2):101–113. doi:10.1097/RMR.0b013e31821e56d8
20. O'Brien JT. Clinical significance of white matter changes. *Am J Geriatr Psychiatry*. 2014;22(2):133–137. doi:10.1016/j.jagp.2013.07.006
21. MacKay A, Whittall K, Adler J, Li D, Paty D, Graeb D. In vivo visualization of myelin water in brain by magnetic resonance. *Magn Reson Med*. 1994;31(6):673–677. doi:10.1002/mrm.1910310614
22. Boa Sorte Silva NC, Dao E, Hsu CL, et al. Myelin content and gait impairment in older adults with cerebral small vessel disease and mild cognitive impairment. *Neurobiol Aging*. 2022;119:56–66. doi:10.1016/j.neurobiolaging.2022.03.020

23. Steinman L. Multiple sclerosis: a coordinated immunological attack against myelin in the central nervous system. *Cell*. 1996;85(3):299–302. doi:10.1016/s0092-8674(00)81107-1
24. Fessel J. Abnormal oligodendrocyte function in schizophrenia explains the long latent interval in some patients. *Transl Psychiatry*. 2022;12(1):120. doi:10.1038/s41398-022-01879-0
25. Bouhrara M, Reiter DA, Bergeron CM, et al. Evidence of demyelination in mild cognitive impairment and dementia using a direct and specific magnetic resonance imaging measure of myelin content. *Alzheimers Dement*. 2018;14(8):998–1004. doi:10.1016/j.jalz.2018.03.007
26. Bouhrara M, Spencer RG. Rapid simultaneous high-resolution mapping of myelin water fraction and relaxation times in human brain using BMC-mcDESPOT. *Neuroimage*. 2017;147:800–811. doi:10.1016/j.neuroimage.2016.09.064
27. Ko S, Ling SM, Winters J, Ferrucci L. Age-related mechanical work expenditure during normal walking: the Baltimore Longitudinal Study of Aging. *J Biomech*. 2009;42(12):1834–1839. doi:10.1016/j.jbiomech.2009.05.037
28. Ferrucci L. The Baltimore Longitudinal Study of Aging (BLSA): a 50-year-long journey and plans for the future. *J Gerontol A Biol Sci Med Sci*. 2008;63(12):1416–1419. doi:10.1093/gerona/63.12.1416
29. Shock N. Normal human aging: the Baltimore Longitudinal Study of Aging. *J Gerontol*. 1985;40(6):767. doi:10.1093/geronj/40.6.767
30. Deoni SC. Transverse relaxation time (T2) mapping in the brain with off-resonance correction using phase-cycled steady-state free precession imaging. *J Magn Reson Imaging*. 2009;30(2):411–417. doi:10.1002/jmri.21849
31. Bouhrara M, Spencer RG. Steady state double angle method for rapid B1 mapping. *Magn Reson Med*. 2019;82(1):189–201. doi:10.1002/mrm.27708
32. Jenkinson M, Beckmann CF, Behrens TE, Woolrich MW, Smith SM. FSL. *Neuroimage*. 2012;62(2):782–790. doi:10.1016/j.neuroimage.2011.09.015
33. Bouhrara M, Spencer RG. Improved determination of the myelin water fraction in human brain using magnetic resonance imaging through Bayesian analysis of mcDESPOT. *Neuroimage*. 2016;127:456–471. doi:10.1016/j.neuroimage.2015.10.034
34. Bouhrara M, Spencer RG. Incorporation of nonzero echo times in the SPGR and bSSFP signal models used in mcDESPOT. *Magn Reson Med*. 2015;74(5):1227–1235. doi:10.1002/mrm.25984
35. Bouhrara M, Reiter DA, Celik H, Fishbein KW, Kijowski R, Spencer RG. Analysis of mcDESPOT- and CPMG-derived parameter estimates for two-component nonexchanging systems. *Magn Reson Med*. 2016;75(6):2406–2420. doi:10.1002/mrm.25801
36. Deoni SC, Rutt BK, Peters TM. Rapid combined T1 and T2 mapping using gradient recalled acquisition in the steady state. *Magn Reson Med*. 2003;49(3):515–526. doi:10.1002/mrm.10407
37. Benjamini Y. Discovering the false discovery rate. *J R Stat Soc Ser B Stat Methodol*. 2010;72(4):405–416. doi:10.1111/j.1467-9868.2010.00746.x
38. Benjamini Y, Hochberg Y. Controlling the false discovery rate: a practical and powerful approach to multiple testing. *J R Stat Soc Ser B Methodol*. 1995;57(1):289–300. doi:10.1111/j.2517-6161.1995.tb02031.x
39. Spencer RG, Bi C. A tutorial introduction to inverse problems in magnetic resonance. *NMR Biomed*. 2020;33(12):e4315. doi:10.1002/nbm.4315
40. Lo OY, Halko MA, Zhou J, Harrison R, Lipsitz LA, Manor B. Gait speed and gait variability are associated with different functional brain networks. *Front Aging Neurosci*. 2017;9:390. doi:10.3389/fnagi.2017.00390
41. Yang FPG, Bal SS, Lee JF, Chen CC. White Matter differences in networks in elders with mild cognitive impairment and Alzheimer's disease. *Brain Connect*. 2021;11(3):180–188. doi:10.1089/brain.2020.0767
42. Sasson E, Doniger GM, Pasternak O, Tarrasch R, Assaf Y. White matter correlates of cognitive domains in normal aging with diffusion tensor imaging. *Front Neurosci*. 2013;7:32. doi:10.3389/fnins.2013.00032
43. Moscufo N, Wolfson L, Meier D, et al. Mobility decline in the elderly relates to lesion accrual in the splenium of the corpus callosum. *Age (Dordr)*. 2012;34(2):405–414. doi:10.1007/s11357-011-9242-4
44. Annweiler C, Schott AM, Montero-Odasso M, et al. Cross-sectional association between serum vitamin D concentration and walking speed measured at usual and fast pace among older women: the EPIDOS study. *J Bone Miner Res*. 2010;25(8):1858–1866. doi:10.1002/jbmr.80
45. Comber L, Galvin R, Coote S. Gait deficits in people with multiple sclerosis: a systematic review and meta-analysis. *Gait Posture*. 2017;51:25–35. doi:10.1016/j.gaitpost.2016.09.026
46. Purcell NL, Goldman JG, Ouyang B, Liu Y, Bernard B, O'Keefe JA. The effects of dual-task cognitive interference on gait and turning in Huntington's disease. *PLoS One*. 2020;15(1):e0226827. doi:10.1371/journal.pone.0226827
47. Fitzpatrick AL, Buchanan CK, Nahin RL, et al.; Ginkgo Evaluation of Memory (GEM) Study Investigators. Associations of gait speed and other measures of physical function with cognition in a healthy cohort of elderly persons. *J Gerontol A Biol Sci Med Sci*. 2007;62(11):1244–1251. doi:10.1093/gerona/62.11.1244
48. Callisaya ML, Launay CP, Srikanth VK, Verghese J, Allali G, Beauchet O. Cognitive status, fast walking speed and walking speed reserve-the Gait and Alzheimer Interactions Tracking (GAIT) study. *Geroscience*. 2017;39(2):231–239. doi:10.1007/s11357-017-9973-y
49. Deshpande N, Metter EJ, Bandinelli S, Guralnik J, Ferrucci L. Gait speed under varied challenges and cognitive decline in older persons: a prospective study. *Age Ageing*. 2009;38(5):509–514. doi:10.1093/ageing/afp093